Current Biology 22, 830–836, May 8, 2012 ©2012 Elsevier Ltd All rights reserved DOI 10.1016/j.cub.2012.03.027

Report

Apoptotic Cells Are Cleared by Directional Migration and *elmo1*-Dependent Macrophage Engulfment

Tjakko J. van Ham,[1,2,3,*] David Kokel,[1,2] and Randall T. Peterson[1,2,*]

[1]Cardiovascular Research Center and Division of Cardiology, Department of Medicine, Massachusetts General Hospital, Harvard Medical School, Charlestown, MA 02129, USA

[2]Broad Institute, 7 Cambridge Center, Cambridge, MA 02142, USA

Summary

Apoptotic cell death is essential for development and tissue homeostasis [1, 2]. Failure to clear apoptotic cells can ultimately cause inflammation and autoimmunity [3, 4]. Apoptosis has primarily been studied by staining of fixed tissue sections, and a clear understanding of the behavior of apoptotic cells in living tissue has been elusive. Here, we use a newly developed technique [5] to track apoptotic cells in real time as they emerge and are cleared from the zebrafish brain. We find that apoptotic cells are remarkably motile, frequently migrating several cell diameters to the periphery of living tissues. F-actin remodeling occurs in surrounding cells, but also within the apoptotic cells themselves, suggesting a cell-autonomous component of motility. During the first 2 days of development, engulfment is rare, and most apoptotic cells lyse at the brain periphery. By 3 days postfertilization, most cell corpses are rapidly engulfed by macrophages. This engulfment requires the guanine nucleotide exchange factor *elmo1*. In *elmo1*-deficient macrophages, engulfment is rare and may occur through macropinocytosis rather than directed engulfment. These findings suggest that clearance of apoptotic cells in living vertebrates is accomplished by the combined actions of apoptotic cell migration and *elmo1*-dependent macrophage engulfment.

Results and Discussion

Apoptotic cells labeled by transgenically expressed, secreted annexin5-YFP (secA5-YFP) were followed by time-lapse confocal imaging during zebrafish brain development [5]. We found that many secA5-YFP$^+$ apoptotic cells arose throughout the embryonic neural tube by 24 hr postfertilization (hpf). These secA5-YFP$^+$ cells persisted for an average of 3 hr without any apparent fragmentation or engulfment. Surprisingly, the apoptotic cells were quite motile, often traveling many cell diameters between their appearance and ultimate lysis (Figure 1A, see also Movie S1 available online). We observed that apoptotic cells typically migrated toward the basolateral side of the neural tube and away from the ventricular, apical side. To investigate this apparent directional preference, we induced high levels of cell death in the brain by treating secA5-YFP;neuronal-mCherry animals with camptothecin, a chemotherapeutic agent, and assessing the apical and basolateral presence of apoptotic cells. Hundreds of apoptotic cells initially emerged at both apical and basolateral positions within the neural tube (Figure 1B and 1C). However, ~9 hr after the camptothecin challenge, few apoptotic cells were present on the apical (ventricular) side of the neural tube, whereas hundreds were detected on the basolateral side of the neural tube (Figure 1B). To quantify directionality, we followed apoptotic cells using 4D tracking and measured displacement of cells over time (Figure 1D). Analysis indicated that the majority of cells followed indirect paths such that their distance traveled exceeded their total displacement. Nevertheless, more than 80% of cells analyzed exhibited a net displacement outward to the basolateral side of the neural tube (Figures 1D and 1E). Therefore, apoptotic cells in the developing brain are highly motile and move almost exclusively in the basolateral direction.

Actinomyosin systems are required for many types of cell movements [6, 7]. To determine whether actinomyosin remodeling is involved in apoptotic cell migration, we treated developing zebrafish with blebbistatin, which uncouples actin-myosin interactions. Blebbistatin treatment rapidly and strongly reduced the motility of apoptotic cells by at least 4-fold (Figures 2A and 2B). These data suggest that polymerized actin remodeling is involved in the migration, but they do not tell us where this actin remodeling actually occurs.

Apoptotic cells in the brain appear to be of two distinct types. Early cells are irregular in shape, motile, and actively blebbing (Figure 2C). They are also surrounded by a thin, smooth secA5-YFP border. Late apoptotic cells are almost perfectly round and are not actively blebbing (Figure 2C). They not only are surrounded by a secA5-YFP border but also exhibit patches of secA5-YFP throughout the cell. Approximately 70% of cells are early, whereas ~30% of cells are late stage (n = 86, data not shown).

Rho-associated protein kinase (ROCK) is known to contribute to cell blebbing and is activated in apoptotic cells [8]. To determine whether ROCK-dependent movement contributes to apoptotic cell migration, we inhibited ROCK activity. The number of blebbing cells in ROCK inhibitor-treated animals was reduced, (data not shown) and velocity of movement was decreased by 50% (Figure 2D). This suggests that the blebbing and motility exhibited by many apoptotic cells is controlled by ROCK.

Previous studies using cultured cells have demonstrated that apoptotic cells can be extruded from epithelial sheets by coordinated contraction of neighboring cells [9–11]. To determine whether this type of extrusion also occurs in the zebrafish, we imaged apoptotic cell movement with higher scan rates to look for evidence of coordinated contraction of neighboring cells. Instead, we observed that apoptotic cells underwent constant curving and blebbing of the plasma membrane, showing large outward membrane bulges that appeared to move between neighboring cells (Figure 1A; Movie S1). This led us to hypothesize that active actinomyosin remodeling occurs within dying cells to drive their migration. To test this hypothesis, we visualized polymerized actin

[3]Present address: Department of Cell Biology, University Medical Center Groningen, University of Groningen, 9700 RB Groningen, The Netherlands

*Correspondence: t.j.van.ham@umcg.nl (T.J.v.H.), peterson@cvrc.mgh.harvard.edu (R.T.P.)

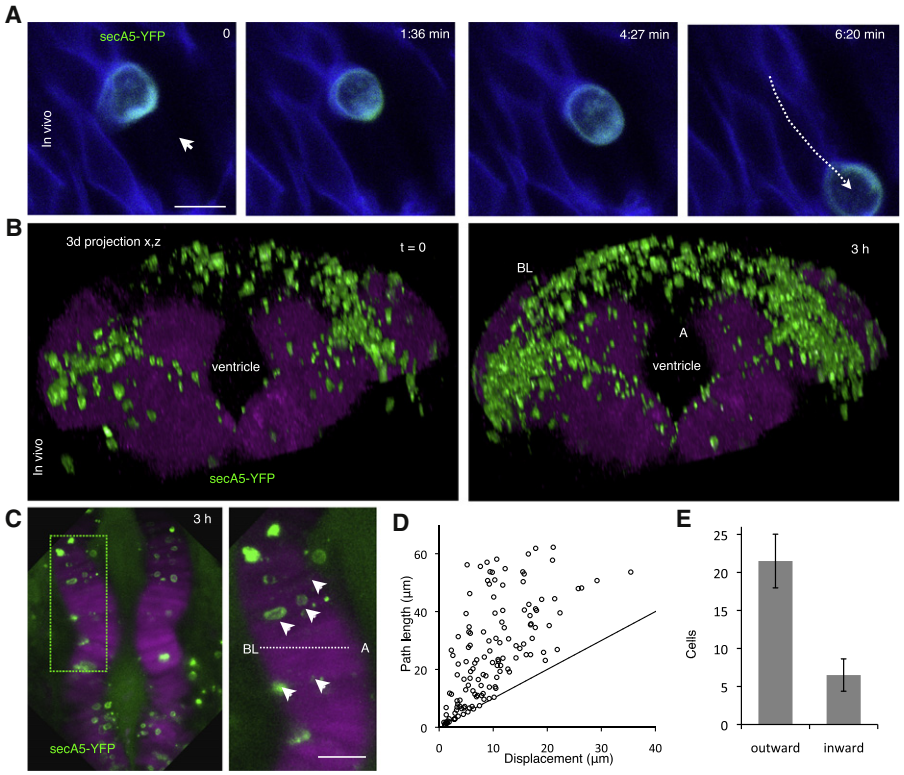

Figure 1. Apoptotic Cells Migrate Directionally

(A) Time-lapse images showing representative apoptotic cell emerging and moving through the neural tube. Apoptotic cell is marked in green (secA5-YFP, arrowhead), and neural tube tissue is marked by membrane-targeted GFP (mGFP, blue). Arrow and dotted line in last frame (6:20) indicates the path traveled by the apoptotic cell.

(B) Images showing secA5-YFP transgenic animals (~30 hpf) treated with a low concentration of camptothecin (50 nM). Neuronal cells are marked with red fluorescent protein. Three-dimensional projections (caudal view) of z stacks were acquired in treated animals at the indicated intervals (apoptotic cells labeled in green, secA5-YFP). First panel (t = 0) is 6 hr after drug treatment when apoptotic cells start to be induced, second panel (t = 3) indicates 3 hr later.

(C) Apoptotic cells (inset, arrowheads) emerge throughout the neural tube, indicating that cell death induction is independent of position in the neural tube. Scale bars represent 5 μm (A) and 25 μm (C).

(D) Plot shows the path length (total distance) and the displacement (net distance traveled) for dying cells. x = y line indicates optimal directional persistence.

(E) Quantification of cells showing net migration outward and inward in the neural tube. Data are represented as mean ± SEM. Also see Figure S1.

(F-actin) using the Lifeact fluorescent probe [12]. Although we occasionally observed high levels of F-actin surrounding late secA5-YFP$^+$ cells, likely in bordering cells, F-actin intensity was cortically enriched within the interior of the majority of early apoptotic cells (Figures 2E–2L). The intensity of internal F-actin changed dynamically with the movement of the apoptotic cells (Movie S2). Together, these findings suggest the possibility of a new mode of apoptotic cell clearance in which these cells contribute to their own removal by actino-myosin-based migration out of the neural tube. It appears that extrusion by contraction of neighboring cells occurs as well, especially at late stages of apoptosis, suggesting that extrusion and migration may operate in the same tissue (Figures 2I–2L; Movie S2, right panels).

After tracking hundreds of apoptotic cells in the brains of 24 hpf zebrafish embryos, we observed little engulfment by macrophages or other cell types. Therefore, directional migration may be the primary means of removing dying cells from the embryonic brain prior to the arrival of macrophages. Directional migration of apoptotic neurons continued to occur even in later stages of development when macrophage engulfment was more widespread. For example, we observed apoptotic cells that migrated out of the neural tube in 5 dpf animals (Figure S1). Therefore, migration of apoptotic cells is not limited to early embryonic development and may contribute to cell corpse clearance in older animals.

Beginning at about 48 hpf, we often observed that apoptotic cells disappeared soon after becoming secA5-YFP positive. To determine whether these cells were disappearing due to engulfment, we tracked dozens of secA5-YFP$^+$ cells at 60 hpf. Immediately before their disappearance, we frequently observed the approach of a large nonneuronal (nonfluorescent) cell that exhibited characteristic dynamics, shape, and behavior of primitive macrophages (Figures 3A–3C; Movie S3).

Primitive macrophages are known to arrive in the brain by 24 hr postfertilization in zebrafish [13, 14]. Loss of the myeloid transcription factor PU.1 or colony-stimulating factor-1 receptor (CSF1R) causes a lack of these primitive macrophages in mice as well as zebrafish [15–20]. Genetic evidence suggests that these macrophages contribute to clearance of apoptotic cells in vivo. However, visualizing the interaction of primitive macrophages with apoptotic cells in vivo has been difficult.

To visualize these engulfing cells with higher resolution, we used bright-field microscopy and confocal imaging of a ubiquitously expressed membrane-localized GFP (memGFP).

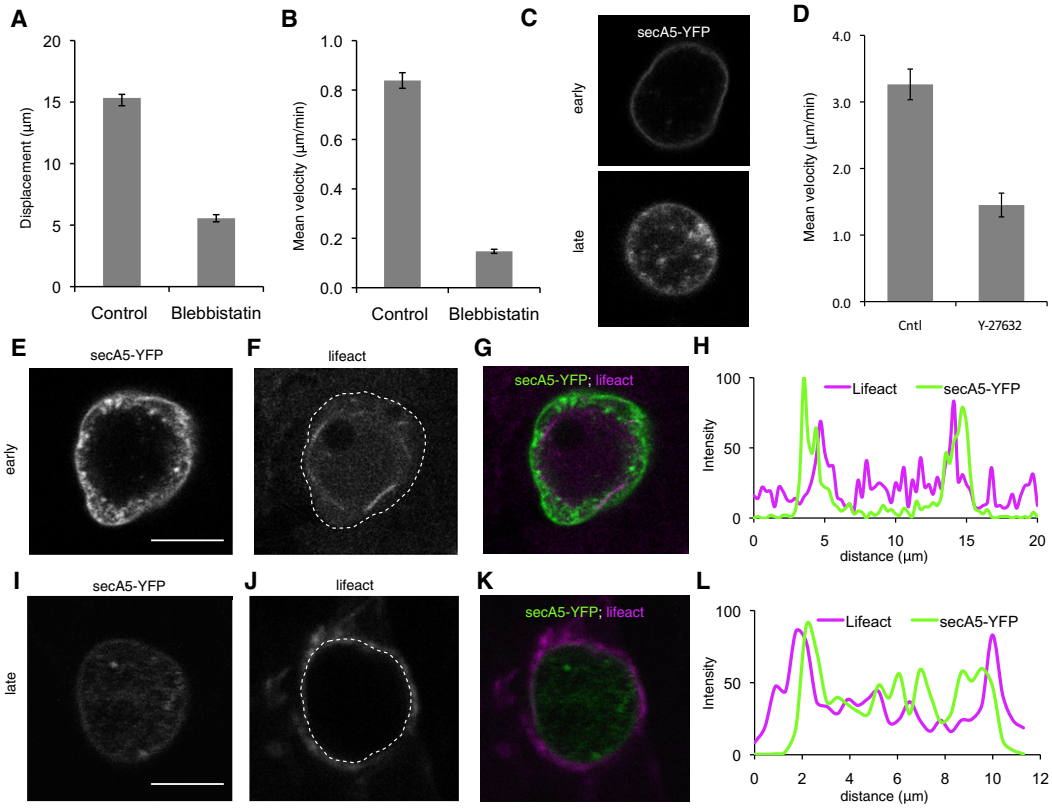

Figure 2. Apoptotic Cells Exhibit Internal Actin Remodeling

(A and B) Quantification of displacement and velocity of apoptotic cells showing strong reduction in both parameters in cpt/blebbistatin versus cpt-only treated animals. Animals were treated with camptothecin (cpt) alone (left) or cotreated with cpt and blebbistatin (right). Images of blebbistatin-treated animals show reduced motility compared to animals treated only with cpt.

(C) Images of motile, blebbing (early) and round, patchy (late) secA5-YFP$^+$ cells.

(D) Quantification of velocity of apoptotic cells in control and Y-27632 (250 μM)-treated animals.

(E–H) Representative early apoptotic cell positive for cortical F-actin as indicated by Lifeact fluorescence. This shows high fluorescence inside the apoptotic cell as determined by the boundary of the annexin signal. Note actin bundles within the cell in (F).

(I–L) Representative late stage apoptotic cell showing high external Lifeact fluorescence surrounding the apoptotic cell, likely within surrounding cells.

(H and L) Quantification of relative fluorescence intensity for secA5-YFP (green) and Lifeact (purple) along a line drawn through the center of the early (H) and late (L) apoptotic cells. Lifeact fluorescence is primarily interior to the annexin signal in early cells and exterior to the annexin signal in late cells. Dotted lines in (F) and (J) indicate outer edge of the cell (as determined by secA5-YFP signal). Scale bars represent 5 μm (E and I). Data are represented as mean ± SEM.

We observed large (diameter > 10 μm), highly motile cells on the yolk and in the brain that possessed long, dynamic cellular processes reminiscent of the ruffles and filopodia characteristic of primitive macrophages (Figures 3D–3F). By 60 hpf, we observed these cells actively foraging along the margins and interior of the neural tube and engulfing secA5-YFP$^+$ cells. The engulfing cells showed a low level of GFP driven by the Fli1 promoter both in a nuclear reporter line and a cytoplasmic reporter line, characteristic of primitive macrophages (Figure 3D) [21]. These cells were also PU.1-GFP positive, and negative for other markers, including the neutrophil marker lysozyme Z (Lyz-dsRed) and microglial marker Apolipoprotein E (ApoE-GFP) [17, 22] (Figure S2). Together, these data suggest that apoptotic cells are engulfed by primitive macrophages at 60 hpf.

To determine whether macrophages are major contributors to cell corpse clearance during brain development, we knocked down the PU.1 transcription factor that controls macrophage differentiation in vertebrates [18, 20, 23]. As expected, knockdown of PU.1 caused an almost complete loss of primitive macrophages (Figure 3J). Numbers of apoptotic cells remained unchanged during the first day of development, indicating that primitive macrophages do not affect cell corpse clearance during early development. By contrast, the number of apoptotic cells in older animals increased approximately 10-fold relative to control animals (Figures 3I and 3K). In the absence of primitive macrophages, apoptotic cells accumulated on the outer edges of the rostralmost part of the forebrain between the telencephalon and olfactory bulbs (Figure 3I). These data suggest that primitive macrophages are responsible for most of the engulfment occurring between 2 and 3 days of development and that in the absence of engulfment, directed migration of apoptotic cells persists in older embryos.

Genetic screens in *C. elegans* and *Drosophila* have elucidated genetic pathways required for cell corpse engulfment [24–26]. Ced-12/*Elmo1* gene is a guanine nucleotide exchange factor (GEF) required for cell corpse engulfment in *C. elegans* [27]. In vertebrates, *ELMO1* is required for engulfment of apoptotic germ cells in the mouse testes by Sertoli cells [28] and was recently found to play a role in neurogenesis in the mouse postnatal brain [29]. However, it is unknown whether *ELMO1* functions in macrophages or other tissues besides

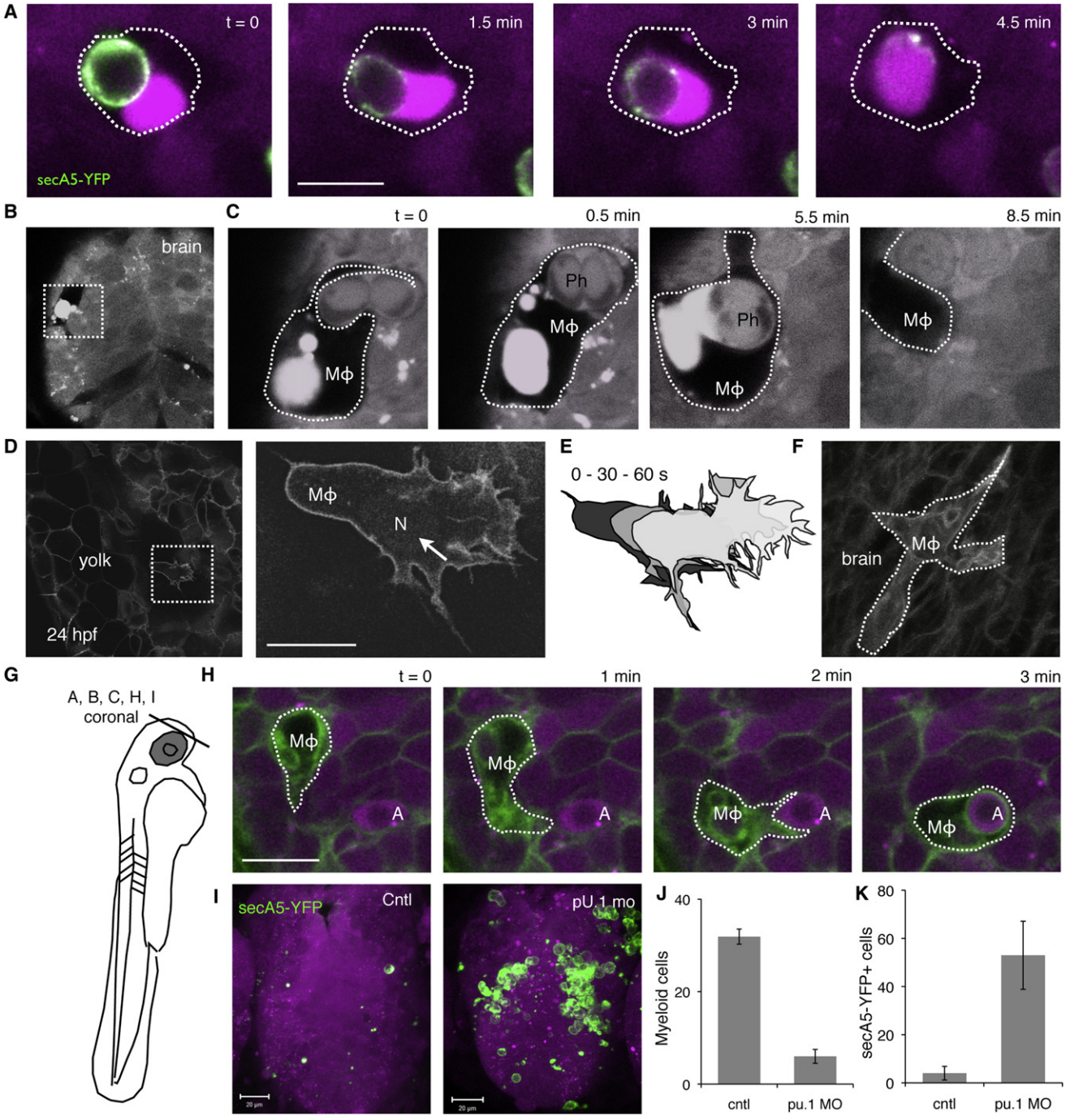

Figure 3. Primitive Macrophages Are Responsible for Engulfment

(A) Engulfed secA5-YFP$^+$ cell fuses with fluorescent vacuole in macrophage.

(B and C) Large vacuole marked by red fluorescent protein originally expressed in neurons and dark surrounding shape indicates presence of macrophage in the forebrain (rostral view).

(D) Image of memGFP transgenic animals showing a large migratory cell on yolk resembling a macrophage. Nuclear Fli1 GFP expression (arrow), a marker for primitive macrophages, is visible in the nucleus (N) of the presumptive macrophage.

(E) Cartoon depicts dynamics of the cell.

(F) memGFP labeled macrophage near the otic vesicle in the hindbrain at 24 hpf.

(G) Drawing of 48 hpf larva, indicating orientation of coronal optical sections shown in (D)–(F), (H), and (I) [38].

(H) Images showing a representative example of a macrophage in the forebrain engulfing an apoptotic cell. Nuclear condensation, characteristic of apoptosis, can be distinguished by the darker spot in fluorescently marked apoptotic cell (marked by "A"). Macrophages are indicated by "Mϕ."

(I) WT (left, Cntl) and PU.1 morphant (right) brains are marked by transgenic expressed red fluorescent protein in secA5-YFP transgenic animals ~60 hpf.

(J) Quantification of macrophages on yolk by memGFP in control and PU.1 morpholino-injected animals.

(K) Quantification of apoptotic cells in forebrain region shown in (I) in control and PU.1 morphants. Data are represented as mean ± SEM in (J) and (K); $p < 0.05$. Scale bars represent 10 μm (A, D, and H). Also see Figure S2.

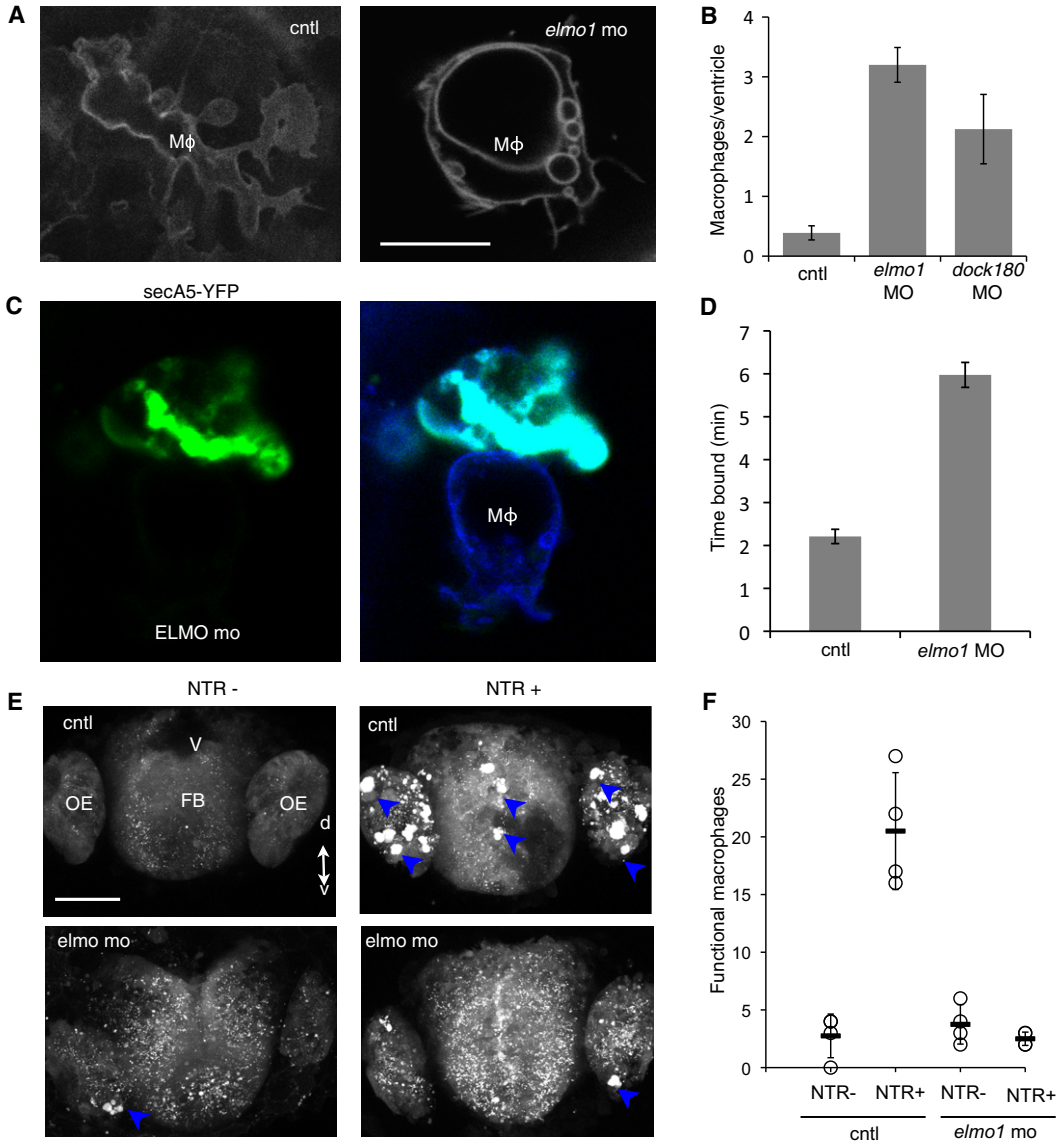

Figure 4. *Elmo1* Controls Engulfment by Primitive Macrophages in Zebrafish

(A) *Elmo1* deficient macrophages show large vacuoles and lack clear polarity seen in WT macrophages. Image shows a representative *elmo1*-deficient macrophage in the ventricle.

(B) Quantification of macropinocytic macrophages inside the ventricle. Data are presented as mean ± SEM (n = 8).

(C) Image showing a macrophage in *elmo1* knockdown larvae bound to a mass of secA5-YFP^{+} apoptotic debris (Movie S4).

(D) Quantification of the time from first encounter of secA5-YFP^{+} cell by a macrophage before being fully engulfed. The time bound for elmo1 MO may be an underestimate because most cells remained unengulfed at the end of the time-lapse observation.

(E) Representative thick optical sections (maximal projections of confocal z stacks) showing fluorescent protein only and NTR;fluorescent protein forebrains of 72 hpf animals treated with metronidazole (1 μM). OE, olfactory epithelium; FB, forebrain; V, ventricle.

(F) Quantification of macrophages as marked by fluorescent vacuoles and high motility, in animals described in (E). Circles indicate individual animals; black bars indicate mean. Macrophages are indicated by "Mϕ" or by blue arrowheads (E), n = 4 animals, error bars represent SEM; $p < 0.05$. Scale bars represent 10 μm (A) and 50 μm (E). Also see Figure S3.

the testes, and if so, how engulfment is affected by defective ELMO signaling.

To determine whether *ELMO1* is necessary for cell corpse engulfment in zebrafish, we analyzed macrophages in *elmo1* knockdown animals at different developmental stages. Migration of primitive macrophages from the yolk into the head mesenchyme ~24 hpf appeared normal as did initial macrophage morphology. However, by 48 hpf, we observed abnormally large macrophages in the brain ventricles of *elmo1* deficient animals. In wild-type (WT) animals, the macrophages in the ventricles were polarized and remained attached to the ventricle roof (Figure 4A). In *elmo1* morphants, these macrophages detached from the ventricle roof and moved freely through the ventricular fluid (Figures 4A and 4C; Movie S4). The *elmo1* deficient macrophages contained many large vacuoles (as large as 10 μm in diameter), and we observed large membrane ruffles capturing surrounding liquid, reminiscent of macropinocytosis (Movie S4).

ELMO/CED-12 functions together with DOCK180/CED-5 to activate Rac1/CED-10 in *C. elegans* engulfment [30]. To verify

conservation and specificity of this pathway, we analyzed macrophages in *dock180* knockdown animals and found a similar increase in macropinocytic macrophages in *dock180* morphant animals (Figure 4B).

To characterize the defect in *elmo1*-deficient animals further, we tracked macrophages and found that they still approached apoptotic cells and bound to them but often failed to engulf them (Figure 4C; Movie S4). On average, it takes 2 min from first encounter of an apoptotic cell to complete engulfment in WT macrophages. In *elmo1*-deficient macrophages, we found that apoptotic cells were still bound to the outside of the macrophage 6 min after initial contact, suggesting a defect in the ability to engulf apoptotic cells (Figure 4D). We frequently observed macrophages in brain ventricles whose exterior surfaces were decorated with apoptotic cells (Figure 4C; Movie S4). Many of these macrophages did have secA5-YFP$^+$ apoptotic material inside them, and occasionally we observed that these decorated macrophages would engulf one of the secA5-YFP$^+$ cells attached to their surface through this macropinocytic process. However, the macropinocytic behavior appeared not to be directed, and the majority of engulfment attempts occurred away from the bound apoptotic cells.

To quantify the engulfment defects we observed in *elmo1*-deficient macrophages, we induced supernumerary apoptotic cells in the brain using the bacterial enzyme nitroreductase (NTR) [31, 32]. Treatment of NTR transgenic animals with metronidazole (met) caused dose-dependent apoptosis of neurons coexpressing NTR and mCherry. In these animals, we observed a >5-fold increase in highly motile macrophages containing large quantities of lysosomal mCherry, suggesting that these macrophages had been actively engulfing apoptotic, mCherry-expressing neurons (Figures 4E and 4F). When comparing *elmo1* morphant NTR versus WT NTR animals, we observed a >5-fold reduction in macrophages that engulfed apoptotic cells in animals deficient in *elmo1* (Figures 4E and 4F). When comparing untreated WT to *elmo1* morphants, we observed increased cellular debris in *elmo1* morphants as marked by small fluorescent apoptotic fragments. Together, these data suggest a sharp decline in macrophage capacity to engulf apoptotic cells in *elmo1* morphants. Knockdown of *dock180* also caused a similar decrease in engulfment capacity, although the effect was less potent, possibly due to lack of sufficient knockdown or redundancy (Figure S3).

One potential explanation for the effect of targeting this engulfment pathway is that lack of *elmo1* causes a defect in directing the formation of a phagocytic cup at the proper position where an apoptotic cell is bound. ELMO1 is thought to be activated by the phosphatidylserine receptor BAI1 and to act as a guanine nucleotide exchange factor for Rac1 [33]. Therefore, *elmo1* may ensure that Rac1-mediated formation of the phagocytic cup occurs at the site of BAI1 activation when a macrophage contacts an apoptotic cell. How an elmo1-deficient macrophage switches into a macropinocytotic mode is not clear, but these cells do occasionally manage to internalize bound apoptotic cells, indicating that elmo1-independent engulfment is rare but can still occur occasionally.

The dramatic macrophage phenotype and engulfment defects we observed in zebrafish were not reported in ELMO1-knockout mice [28]. This may be due to functional redundancy with other ELMO genes in mice. Alternatively, engulfment defects may have been missed by a lack of in vivo methods to visualize engulfment with sufficient spatiotemporal resolution. Indeed, a more recent study shows a potential role for *elmo1* in neighboring cell engulfment in the mouse subventricular zone [29].

It has been noted that annexin-5 inhibits engulfment in an in vitro flow-cytometry-based phagocytosis assay [34]. Although we cannot eliminate the possibility of a minor inhibition of engulfment by secA5-YFP in vivo, it is clear that secA5-YPF-positive cells are efficiently recognized and engulfed (in an average of 2 min—see Figure 4D) by macrophages in vivo.

It is interesting to speculate on the advantages of employing two distinct methods of apoptotic cell clearance—migration and engulfment. Prior to macrophages becoming functional, directional migration provides a means of removing cells to the central nervous system (CNS) periphery, where eventual cell lysis is less likely to interfere with brain function or cause inflammation. But even after macrophages become active, apoptotic cell migration out of the neural tube continues. It is possible that migration and extrusion might direct apoptotic cells to areas in the brain more easily accessible for phagocytes. In line with such a mechanism, *Drosophila* macrophages rarely enter tissues and seem mainly to scavenge intertissue spaces for apoptotic cells [35]. Additionally, in immunohistochemistry and EM studies of developmental cell death, apoptotic cells accumulate on the periphery of the CNS in *Drosophila* lacking engulfment [36]. Therefore, in addition to being a disposal method in its own right, directed migration of apoptotic cells may facilitate engulfment by macrophages and limit the extent to which macrophages must invade sensitive tissues to find apoptotic cells.

The studies described here have focused on clearance of apoptotic cells from the developing zebrafish brain. It is possible, although untested, that apoptotic cell migration and *elmo1*-dependent engulfment contribute to apoptotic cell clearance in other developing organs and adult tissues. Because some organs must deal with the clearance of billions of cells that die every day [37], the mechanisms of apoptotic cell disposal described here may be relevant to understanding conditions ranging from autoimmune disease to chronic inflammation.

Experimental Procedures

All zebrafish experiments were conducted with approval of the Massachusetts General Hospital Institutional Animal Care and Use committee. For additional experimental procedures, see the Supplemental Information.

Supplemental Information

Supplemental Information includes three figures, Supplemental Experimental Procedures, and four movies and can be found with this article online at doi:10.1016/j.cub.2012.03.027.

Acknowledgments

We thank the members of the Peterson laboratory for helpful discussion and Kristin White and Iain Drummond for helpful discussion and critical reading of the manuscript. We thank John Kanki, Marnie Halpern, Francesca Peri, Chetana Sachidanandan, and Reinhard Köster for transgenic zebrafish and Erez Raz and Roland Wedlich-Söldner for providing Lifeact reagents. This work was supported by National Institutes of Health grants NS063733 (R.T.P.), MH086867 (R.T.P.) and K01MH091449 (D.K.) and by the Charles and Ann Sanders MGH Research Scholar Award.

Received: November 10, 2011
Revised: February 14, 2012
Accepted: March 16, 2012
Published online: April 12, 2012

References

1. Buss, R.R., Sun, W., and Oppenheim, R.W. (2006). Adaptive roles of programmed cell death during nervous system development. Annu. Rev. Neurosci. *29*, 1–35.
2. Glucksmann, A. (1951). Cell deaths in normal vertebrate ontogeny. Biol. Rev. Camb. Philos. Soc. *26*, 59–86.
3. Nagata, S., Hanayama, R., and Kawane, K. (2010). Autoimmunity and the clearance of dead cells. Cell *140*, 619–630.
4. Savill, J., Dransfield, I., Gregory, C., and Haslett, C. (2002). A blast from the past: clearance of apoptotic cells regulates immune responses. Nat. Rev. Immunol. *2*, 965–975.
5. van Ham, T.J., Mapes, J., Kokel, D., and Peterson, R.T. (2010). Live imaging of apoptotic cells in zebrafish. FASEB J. *24*, 4336–4342.
6. Fackler, O.T., and Grosse, R. (2008). Cell motility through plasma membrane blebbing. J. Cell Biol. *181*, 879–884.
7. Kardash, E., Reichman-Fried, M., Maitre, J.L., Boldajipour, B., Papusheva, E., Messerschmidt, E.M., Heisenberg, C.P., and Raz, E. A role for Rho GTPases and cell-cell adhesion in single-cell motility in vivo. Nat. Cell Biol. *12*, 47–53.
8. Sebbagh, M., Renvoizé, C., Hamelin, J., Riché, N., Bertoglio, J., and Bréard, J. (2001). Caspase-3-mediated cleavage of ROCK I induces MLC phosphorylation and apoptotic membrane blebbing. Nat. Cell Biol. *3*, 346–352.
9. Rosenblatt, J., Raff, M.C., and Cramer, L.P. (2001). An epithelial cell destined for apoptosis signals its neighbors to extrude it by an actin- and myosin-dependent mechanism. Curr. Biol. *11*, 1847–1857.
10. Sträter, J., Koretz, K., Günthert, A.R., and Möller, P. (1995). In situ detection of enterocytic apoptosis in normal colonic mucosa and in familial adenomatous polyposis. Gut *37*, 819–825.
11. Wang, F., Wang, F., Zou, Z., Liu, D., Wang, J., and Su, Y. (2011). Active deformation of apoptotic intestinal epithelial cells with adhesion-restricted polarity contributes to apoptotic clearance. Lab. Invest. *91*, 462–471.
12. Riedl, J., Crevenna, A.H., Kessenbrock, K., Yu, J.H., Neukirchen, D., Bista, M., Bradke, F., Jenne, D., Holak, T.A., Werb, Z., et al. (2008). Lifeact: a versatile marker to visualize F-actin. Nat. Methods *5*, 605–607.
13. Herbomel, P., Thisse, B., and Thisse, C. (1999). Ontogeny and behaviour of early macrophages in the zebrafish embryo. Development *126*, 3735–3745.
14. Lichanska, A.M., and Hume, D.A. (2000). Origins and functions of phagocytes in the embryo. Exp. Hematol. *28*, 601–611.
15. Ginhoux, F., Greter, M., Leboeuf, M., Nandi, S., See, P., Gokhan, S., Mehler, M.F., Conway, S.J., Ng, L.G., Stanley, E.R., et al. (2010). Fate mapping analysis reveals that adult microglia derive from primitive macrophages. Science *330*, 841–845.
16. Herbomel, P., Thisse, B., and Thisse, C. (2001). Zebrafish early macrophages colonize cephalic mesenchyme and developing brain, retina, and epidermis through a M-CSF receptor-dependent invasive process. Dev. Biol. *238*, 274–288.
17. Hsu, K., Traver, D., Kutok, J.L., Hagen, A., Liu, T.X., Paw, B.H., Rhodes, J., Berman, J.N., Zon, L.I., Kanki, J.P., and Look, A.T. (2004). The pu.1 promoter drives myeloid gene expression in zebrafish. Blood *104*, 1291–1297.
18. McKercher, S.R., Torbett, B.E., Anderson, K.L., Henkel, G.W., Vestal, D.J., Baribault, H., Klemsz, M., Feeney, A.J., Wu, G.E., Paige, C.J., and Maki, R.A. (1996). Targeted disruption of the PU.1 gene results in multiple hematopoietic abnormalities. EMBO J. *15*, 5647–5658.
19. Pollard, J.W. (1997). Role of colony-stimulating factor-1 in reproduction and development. Mol. Reprod Dev. *46*, 54–60.
20. Scott, E.W., Simon, M.C., Anastasi, J., and Singh, H. (1994). Requirement of transcription factor PU.1 in the development of multiple hematopoietic lineages. Science *265*, 1573–1577.
21. Lawson, N.D., and Weinstein, B.M. (2002). In vivo imaging of embryonic vascular development using transgenic zebrafish. Dev. Biol. *248*, 307–318.
22. Peri, F., and Nüsslein-Volhard, C. (2008). Live imaging of neuronal degradation by microglia reveals a role for v0-ATPase a1 in phagosomal fusion in vivo. Cell *133*, 916–927.
23. Rhodes, J., Hagen, A., Hsu, K., Deng, M., Liu, T.X., Look, A.T., and Kanki, J.P. (2005). Interplay of pu.1 and gata1 determines myelo-erythroid progenitor cell fate in zebrafish. Dev. Cell *8*, 97–108.
24. Reddien, P.W., and Horvitz, H.R. (2004). The engulfment process of programmed cell death in caenorhabditis elegans. Annu. Rev. Cell Dev. Biol. *20*, 193–221.
25. Krieser, R.J., and White, K. (2002). Engulfment mechanism of apoptotic cells. Curr. Opin. Cell Biol. *14*, 734–738.
26. Elliott, M.R., and Ravichandran, K.S. (2010). Clearance of apoptotic cells: implications in health and disease. J. Cell Biol. *189*, 1059–1070.
27. Gumienny, T.L., Brugnera, E., Tosello-Trampont, A.C., Kinchen, J.M., Haney, L.B., Nishiwaki, K., Walk, S.F., Nemergut, M.E., Macara, I.G., Francis, R., et al. (2001). CED-12/ELMO, a novel member of the CrkII/Dock180/Rac pathway, is required for phagocytosis and cell migration. Cell *107*, 27–41.
28. Elliott, M.R., Zheng, S., Park, D., Woodson, R.I., Reardon, M.A., Juncadella, I.J., Kinchen, J.M., Zhang, J., Lysiak, J.J., and Ravichandran, K.S. (2010). Unexpected requirement for ELMO1 in clearance of apoptotic germ cells in vivo. Nature *467*, 333–337.
29. Lu, Z., Elliott, M.R., Chen, Y., Walsh, J.T., Klibanov, A.L., Ravichandran, K.S., and Kipnis, J. Phagocytic activity of neuronal progenitors regulates adult neurogenesis. Nat. Cell Biol. *13*, 1076–1083.
30. Kiyokawa, E., Hashimoto, Y., Kobayashi, S., Sugimura, H., Kurata, T., and Matsuda, M. (1998). Activation of Rac1 by a Crk SH3-binding protein, DOCK180. Genes Dev. *12*, 3331–3336.
31. Pisharath, H., Rhee, J.M., Swanson, M.A., Leach, S.D., and Parsons, M.J. (2007). Targeted ablation of beta cells in the embryonic zebrafish pancreas using E. coli nitroreductase. Mech. Dev. *124*, 218–229.
32. Davison, J.M., Akitake, C.M., Goll, M.G., Rhee, J.M., Gosse, N., Baier, H., Halpern, M.E., Leach, S.D., and Parsons, M.J. (2007). Transactivation from Gal4-VP16 transgenic insertions for tissue-specific cell labeling and ablation in zebrafish. Dev. Biol. *304*, 811–824.
33. Park, D., Tosello-Trampont, A.C., Elliott, M.R., Lu, M., Haney, L.B., Ma, Z., Klibanov, A.L., Mandell, J.W., and Ravichandran, K.S. (2007). BAI1 is an engulfment receptor for apoptotic cells upstream of the ELMO/Dock180/Rac module. Nature *450*, 430–434.
34. Kenis, H., van Genderen, H., Deckers, N.M., Lux, P.A., Hofstra, L., Narula, J., and Reutelingsperger, C.P. (2006). Annexin A5 inhibits engulfment through internalization of PS-expressing cell membrane patches. Exp. Cell Res. *312*, 719–726.
35. Abrams, J.M., White, K., Fessler, L.I., and Steller, H. (1993). Programmed cell death during Drosophila embryogenesis. Development *117*, 29–43.
36. Sonnenfeld, M.J., and Jacobs, J.R. (1995). Apoptosis of the midline glia during Drosophila embryogenesis: a correlation with axon contact. Development *121*, 569–578.
37. Croft, D.N., Loehry, C.A., Taylor, J.F., and Cole, J. (1968). DNA and cell loss from normal small-intestinal mucosa. Lancet *292*, 70–73.
38. Kimmel, C.B., Ballard, W.W., Kimmel, S.R., Ullmann, B., and Schilling, T.F. (1995). Stages of embryonic development of the zebrafish. Dev. Dyn. *203*, 253–310.